Groundwater chemistry and health risks associated with nitrate intake in Hailun, northeast China

Tian Hui, Sun Qifa, Kang Zhuang, Li Xuguang, Du Jizhong and Jin Hongtao

ABSTRACT

In order to quantify the hydrochemical characteristics of groundwater in Hailun, analyze the hydrochemical process, and evaluate its health risks associated with nitrate intake, 77 shallow groundwater samples were collected and analyzed. The results show that groundwater in the study area is weakly acidic and groundwater chemical type was dominated by HCO_3-Ca, HCO_3•Cl-Ca, HCO_3-Ca•Na and HCO_3•Cl-Ca•Na. Rock weathering and dissolution, ion exchange, and human activities are the main reasons affecting the chemical composition of shallow groundwater in Hailun. The weathering and dissolution process of silicate under weakly alkaline conditions is the source of Na. The dissolution of calcite, dolomite, and gypsum are the main form of water–rock interaction. Results of health risk assessment show that the HQ value for adult males, adult females, children, and infants were in range of 0–1.52, 0–1.75, 0–3.58 and 0–6.08, respectively, and with a mean value of 0.19, 0.22, 0.44, 0.75, respectively. The harm of NO_3 pollution is in the order of infant > child > adult female > adult male. The results of this study made local governments pay attention to drinking water safety issues for local residents.

Key words | China, groundwater chemistry, health risk assessment, nitrogen

Tian Hui
Sun Qifa
Kang Zhuang (corresponding author)
Li Xuguang
Du Jizhong
Jin Hongtao
Shenyang Geological Survey Center,
China Geological Survey,
Shenyang 110034,
China
E-mail: *359585977@qq.com*

Tian Hui
Key Laboratory of Groundwater Resources and Environment, Ministry of Education,
Jilin University,
Changchun 130021,
China
and
College of New Energy and Environment,
Jilin University,
Changchun 130021,
China

HIGHLIGHTS

- In order to quantify the hydrochemical characteristics of groundwater in Hailun, analyze the hydrochemical process, and evaluate its health risks associated with nitrate intake, 77 shallow groundwater samples were collected and analyzed.
- The special purpose of this study is to: (1) explore the hydrochemical characteristics of groundwater; (2) understand the evolution of groundwater and the sources of major ions through factor analysis and hydrochemical analysis; (3) use the parameters recommended in the USEPA2004 guidelines and the HHRA model assesses the health risks of groundwater as drinking water.
- For the first time, the study population was divided into four categories: adult males, adult females, children and infants.
- The health risks of nitrate intake by different genders and age groups were studied. It is expected that the health risks of nitrate intake by different genders and ages can be obtained.
- The results of the study will help local governments strengthen management and governance in places where the groundwater environment is fragile, thereby effectively improving the quality of drinking water for local residents.

doi: 10.2166/wh.2020.050

INTRODUCTION

Groundwater is one of the most precious resources on the planet (Jha *et al.* 2007). It can meet the needs of human survival and development, including for living and drinking, agricultural irrigation, industrial production, etc. (Peiyue *et al.* 2011). However, over the past three decades, due to the rapid development of agricultural modernization in China, the demand for groundwater has been increasing (Chen *et al.* 2018). As a result, a series of environmental geological problems have emerged, such as aquifer drying (Rizeei *et al.* 2019), land subsidence (Raeisi *et al.* 2018), seawater intrusion (Yang *et al.* 2019), soil secondary salinization (Qiu *et al.* 2017), nitrate pollution (Li *et al.* 2016) and wetland degradation (Zhu *et al.* 2015). Among these hazards, nitrate pollution has attracted much attention from the social and scientific communities, mainly because it adversely impacts human health. According to studies, NO_3-N in water has a greater harmful effect on humans and aquatic organisms. Methaemoglobinemia occurs when water with a nitrate content greater than 10 mg/L is drunk for a period of time (Jones *et al.* 2019). If the methemoglobin content in the blood is 70 mg/L, choking can occur (De Roos *et al.* 2003). Nitrate intake from drinking water is a risk factor for colon or rectal cancer (DellaValle *et al.* 2014). The above studies are based on the dietary and drinking water intake of nitrate (Schullehner *et al.* 2018).

Health risk assessment of groundwater is essential. Common pollutants in groundwater include fluoride (F^-), nitrate (NO_3^--N), ammonia nitrogen (NH_4-N), nitrite (NO_2^--N), and heavy metals (Ma *et al.* 2016; Zhang *et al.* 2018). Su *et al.* (2013) evaluated the health risks of nitrate nitrogen in groundwater in agricultural wastewater irrigation areas in northeast China, and the results of the study were that the health risks in urban areas were lower than that of agricultural irrigation areas. Health risk assessments successfully compared the risk between adults and children (Su *et al.* 2013). Zhai *et al.* (2017) evaluated the health risks of nitrate nitrogen in groundwater in the northeast Plain. The results of the study were that the NO_3 concentration in the southeast and northeast of the study area was the highest (Zhai *et al.* 2017). Li *et al.* (2014) calculated the health risks of nitrate nitrogen in groundwater in the industrial park in northwest China, and the research results show that the annual health risk is higher than the highest acceptable level recommended by the International Commission on Radiological Protection.

The Songnen Plain is China's most important commodity grain production base. Hailun is an important part of the northeast of the Songnen Plain and plays an important role in agricultural production. Since 1995, cereal production, especially rice production, has increased significantly (Luo *et al.* 2018). At the same time, with the increase of rice yield, the area irrigated by groundwater rapidly increased. Because surface water is far from meeting the needs of human agricultural production, farmers have to extract groundwater from aquifers for dryland irrigation. However, the hydrogeochemical characteristics of groundwater and drinking water quality in agricultural irrigation areas (Hailun) are still not very clear. This may limit the protection and proper use of groundwater resources, especially drinking water safety issues for local residents.

The purpose of this research can be summarized as: (1) explore the hydrochemical characteristics of groundwater; (2) understand the evolution of groundwater and the sources of major ions through factor analysis and hydrochemical analysis; (3) use the HHRA model to assess the health risks of groundwater as drinking water, with the parameters recommended in the USEPA (2004) guidelines. For the first time, the study population was divided into four categories: adult males, adult females, children and infants. The health risks of nitrate intake by different genders and age groups were studied. It is expected that the health risks of nitrate intake by different genders and ages can be obtained. The results of the study will help local governments strengthen management and governance in places where the groundwater environment is fragile, thereby effectively improving the quality of drinking water for local residents.

STUDY AREA

Study area description

The study region is located in the central part of Heilongjiang Province in northeast China, encompassing an area of 4,668 km^2 between the latitudes of 46°58′E and 47°52′E

and longitudes of 126°14′N and 127°45′N (Figure 1). The study area included Helen city and 23 towns, with a total population of approximately 799,838. Because it is located in the mid-latitudes of the northern hemisphere and belongs to a temperate continental semi-humid monsoon climate, the four seasons are distinctive. Rainfall is mainly concentrated in June–August, with an average annual rainfall of about 600 mm and an average annual temperature of 1–2 °C (Li *et al.* 2018). The elevation is higher in the northeast, and east, but is lower in the west, and southwest, with elevations ranging from 190 to 450 m above mean sea level. There are four types of landforms in the study area, including valleys and floodplains in the west, sloping plains in the middle, hilly areas in the northeast, and high plains in the east. Although the Hailun River, Zhayin River, and Sandaowulong River pass through the area, the seasonal variations in surface water are not suitable for agricultural production. In dry periods, when rivers are low and cannot meet the needs of agricultural production, large areas of groundwater are usually extracted for irrigation.

The flow direction of groundwater is consistent with the trend of terrain and the flow direction of surface water, which is from northeast to southwest. The distribution of groundwater resources is uneven, showing a pattern of scarcity in the east and north, and abundance in the west and south. In the western plains, groundwater resources are relatively abundant. Quaternary diving, confined water and Cretaceous confined water are the main mining layers in this area (Zhang *et al.* 2017). The groundwater level ranged from 5 to 15 m in the dry season. Under normal circumstances, the water output of a single well is 300–500 m^3/day. In the high plains in the east and the hilly areas in the northeast, the Cretaceous confined water and bedrock fissure water develop, but its water output is generally less than 200 m^3/day.

MATERIALS AND METHODS

Sampling and measurements

According to the research plan, from June 2019 to October 2019, 77 shallow groundwater samples were collected in two batches. Shallow groundwater samples were taken from wells used primarily for water supply and irrigation in rural areas. Generally, the depth of water wells is less than 50 m, and their distribution is shown in Figure 1. The spatial distribution of sampling points is not uniform, but is consistent with the distribution of each village, which can objectively reflect the characteristics of groundwater mining status in the study area. In the process of sampling, it is performed in accordance with the sample collection specifications of the China Geological Survey. Each sampling well must be cleaned by pumping water for more than 10 minutes in accordance with groundwater sampling guidelines. Sampling is mainly divided into three steps. The first step is to rinse the vial with well water three times, then fill with water and seal. In the second step, the groundwater sample is stored in a 4 °C incubator. The third step is to return the sample to a qualified laboratory for testing.

In this study, groundwater samples were tested in the laboratory of the Shenyang Institute of Geology and Mineral Resources which has the groundwater testing qualification issued by China.

The laboratory test index includes pondus Hydrogenii (pH), total dissolved solids (TDS), calcium (Ca^{2+}), magnesium (Mg^{2+}), potassium (K^{+}), sodium (Na^{+}), chloride (Cl^{-}), sulfate (SO_4^{2-}), bicarbonate (HCO_3^{-}), nitrate (NO_3^{-}), nitrite (NO_2^{-}) and ammonium (NH_4^{+}). TDS and pH were measured in the field using a calibrated multi-parameter water quality analyzer (HACH-HQ40D). The concentrations of major cations (Ca, Na, K, Mg) were determined in the laboratory using plasma spectroscopy (ICP-6300), and the concentration of major anions (HCO_3, Cl, SO_4, and NO_3) were determined in the laboratory using ion chromatography (ICS-3000). The concentration of NO_2 and NH_4 were obtained using gas phase molecular absorption spectrometry (GMA-3376).

Human Health Risk Assessment (HHRA) model

The Human Health Risk Assessment (HHRA) model is an assessment method for assessing the risks of the various elements in groundwater to human health. It describes the degree of harm to the human body under oral and skin exposure pathways, and proposes recommendations to protect human health (Tian *et al.* 2019). The HHRA is based on four steps: (1) Hazard identification; (2) Dose-response

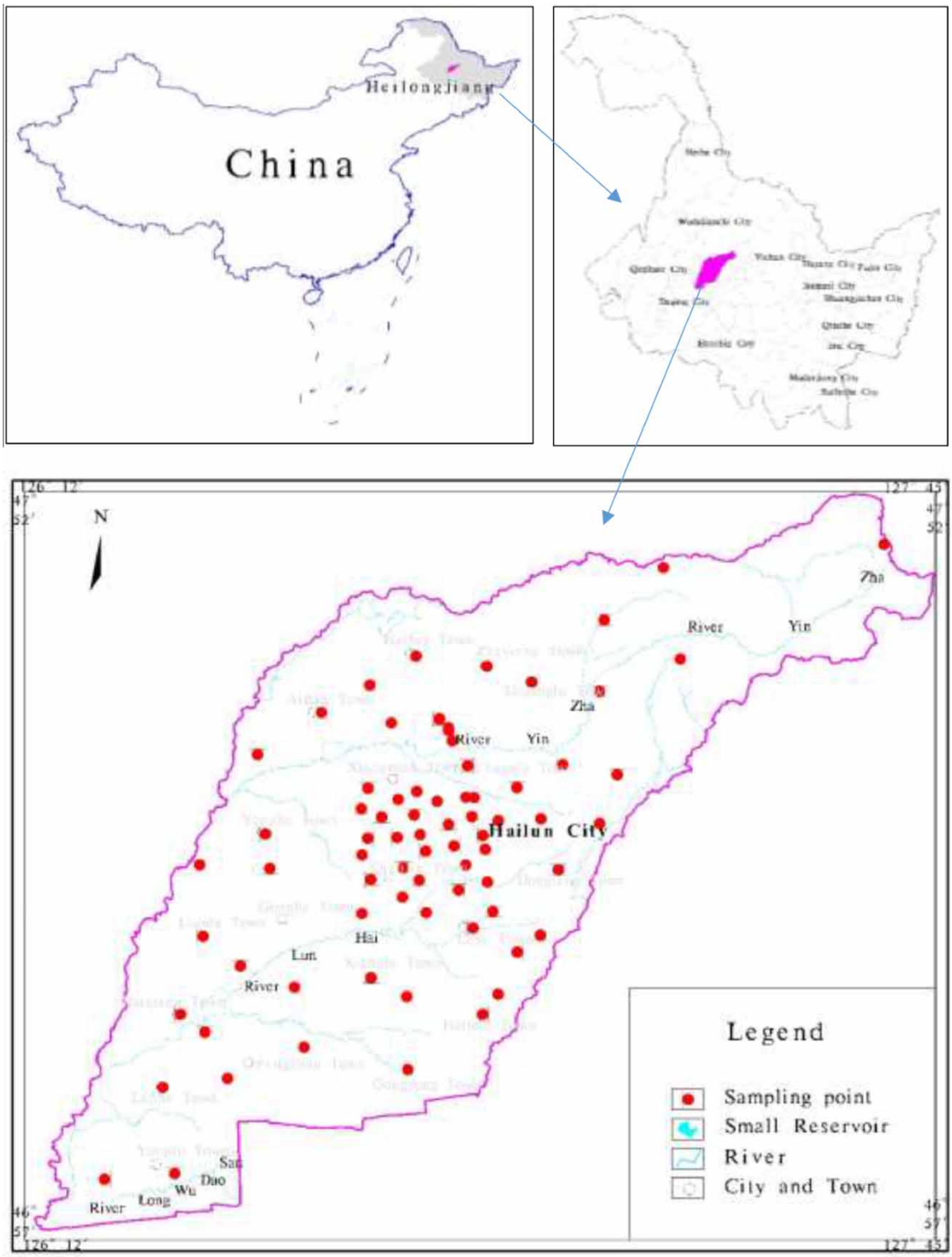

Figure 1 | Location and sampling points of the study area.

assessment; (3) Exposure assessment; (4) Risk characterization (Adimalla *et al.* 2019a, 2019b).

Step 1: Hazard identification (Tian *et al.* 2020a, 2020b). The purpose of hazard identification is to determine the nature and intensity of the source of the risk. This method of assessment requires the collection of a large amount of data, including detailed data on the geography, population, economic development, geology, meteorology, and hydrogeology of the study area.

Step 2: Dose-response assessment (Ford *et al.* 2017):

$$\mathrm{RfD} = (\mathrm{NOAEL(LOAEL)})/\mathrm{UFs} \quad (1)$$

where RfD represents the chronic reference dose (mg/kg/d), NOAEL represents the No Observed Adverse Effect Level (mg/kg/d), LOAEL represents the Lowest Observed Adverse Effect Level (mg/kg/d), UFs represents the uncertainty factors.

Step 3: Exposure assessment (Zhai *et al.* 2017):

$$\mathrm{CDI_{ing-nc}} = \frac{\mathrm{Cw} \times \mathrm{IRW} \times \mathrm{EF} \times \mathrm{ED}}{BW \times \mathrm{AT}} \quad (2)$$

$$\mathrm{CDI_{derm-nc}} = \frac{\mathrm{DA}_{event} \times \mathrm{SA} \times \mathrm{EF} \times \mathrm{ED} \times \mathrm{EV}}{\mathrm{BW} \times \mathrm{AT}} \quad (3)$$

$$\mathrm{DA_{event}} = \mathrm{Kp} \times \mathrm{Cw} \times \mathrm{ET} \times \mathrm{CF} \quad (4)$$

The meanings and assignment of the different parameters for Health Risk Assessment are summarized in Table 1.

Step 4: Risk characterization (Kumar *et al.* 2019).

$$\mathrm{HQ_{ing}} = \frac{CDI_{ing-nc}}{RfD_{ing}} \quad (5)$$

$$\mathrm{HQ_{derm}} = \frac{CDI_{derm-nc}}{RfD_{derm}} \quad (6)$$

$$\mathrm{RfD_{derm}} = \mathrm{RfD_{ing}} \times \mathrm{GIABS} \quad (7)$$

$$\mathrm{HQ_{total}} = \mathrm{HQ_{ing}} + \mathrm{HQ_{derm}} \quad (8)$$

where $\mathrm{HQ_{ing}}$ indicates a non-carcinogenic hazard by ingestion of water (non-dimensional), $\mathrm{HQ_{derm}}$ indicates a non-carcinogenic hazard through dermal absorption of water (non-dimensional). If the HQ exceeds 1, there may be a potential non-carcinogenic effect in humans (Tian *et al.* 2020a, 2020b). If the HQ value is less than 1, this indicates that no non-carcinogenic risk is caused from any substance in the water.

Software

This article mainly uses SPSS software and MapGIS software for analysis and research. SPSS19.0 is used for factor analysis, principal component analysis and statistical analysis of ion concentration. MapGIS software (version 6.7) is a geographic information system software platform. MAPGIS is used to draw geographic location maps, sample distribution maps, hydrochemical-type maps, ion concentration spatial distribution maps, and groundwater EWQI evaluation maps.

RESULTS AND DISCUSSION

The groundwater chemistry is mainly affected by both natural and human factors. Natural factors include regional hydrogeological conditions, chemical composition of precipitation, evaporation and concentration, ion exchange, weathering and dissolution of rocks. Human factors include over-exploitation of groundwater, sewage recharge, pesticide use and fertilizer use.

Physicochemical characteristics

The results of statistical analysis of the physical and chemical indexes of the groundwater samples in the study area are shown in Table 2. The pH range of groundwater samples ranged from 6.14 to 7.60, with a mean value of 6.93. The pH value indicates that the groundwater environment in the study area is weakly acidic. According to WHO guidelines, the permissible value for drinking water is in the pH range of 6.5–8.5. TDS indicates total solids dissolved in the groundwater. According to WHO guidelines, the TDS value of the groundwater for drinking should be less than 500 mg/L. In the groundwater of the study area, the TDS value ranged from 98.91 to 1,920.13 mg/L, with a mean value of 561.81 mg/L. The highest concentration of TDS is

Table 1 | Summary of parameters used to calculate chronic daily intake

Exposure route/exposure factor	Symbol	Value	Units	Reference/source
Water ingestion rate – adult	IRWa	2	L/day	Harries & Harper (2004); Rani *et al.* (2013)
Water ingestion rate – child	IRWc	1	L/day	Harries & Harper (2004)
Exposure frequency	EF	365	days/year	Duggal *et al.* (2013)
Exposure duration – adult	EDa	70	Year	Harries & Harper (2004)
Exposure duration – child	EDc	6	Year	Harries & Harper (2004)
Body weight – adult	BWa	70	Kg	Harries & Harper (2004); Rani *et al.* (2013)
Body weight – child	BWc	15	Kg	Harries & Harper (2004)
Average time – adult	ATa	25,550	Days	$AT = EF \times ED$
Average time – child	ATc	2,190	Days	$AT = EF \times ED$
Absorbed dose per event	DAevent	Calculated value	mg/cm^2-event	Equation (3)
Exposure time – adult	ETa	0.58	Hours/day	USEPA (2004)
Exposure time – child	ETc	1	Hours/day	USEPA (2004)
Event frequency – adult	EVa	1	Event/day	USEPA (2004)
Event frequency – child	EVc	1	Event/day	USEPA (2004)
Skin surface area – adult	SAa	18,000	cm^2	USEPA (2004)
Skin surface area – child	SAc	6,600	cm^2	USEPA (2004)
Conversion factor	CF	0.001	L/cm^3	$1\ L = 1{,}000\ cm^3$
Dermal permeability coefficient	Kp	Contaminant of potential concern (COPC)-specific	cm/hour	USDOE (2011)
Gastrointestinal absorption factor	GIABS	COPC-specific	Unitless	USDOE (2011)
Reference dose-ingestion/dermal	RfDing/derm	COPC-specific	mg/kg/day	USDOE (2011)

Table 2 | Statistics of the measured parameters for groundwater samples

	Parameters	Unit	Minimum	Maximum	Mean	SD	CV(%)
Shallow GW	pH	–	6.14	7.60	6.93	0.35	5.07
	TDS	mg/L	98.91	1,920.13	561.81	396.26	70.53
	Ca^{2+}	mg/L	16.12	315.00	106.01	70.65	66.64
	Mg^{2+}	mg/L	3.75	70.37	23.72	14.15	59.65
	K^+	mg/L	0.76	41.17	3.95	6.75	171.05
	Na^+	mg/L	4.90	215.97	35.23	37.26	105.75
	Cl^-	mg/L	0.13	317.38	87.01	89.58	102.95
	SO_4^{2-}	mg/L	0.21	448.97	62.97	80.78	128.29
	HCO_3^-	mg/L	34.67	809.00	249.79	126.41	50.61
	NO_3-N	mg/L	0.0000	112.42	14.32	24.26	169.43
	NO_2-N	mg/L	0.0000	2.23	0.09	0.28	324.28
	NH_4-N	mg/L	0.0000	4.01	0.18	0.58	314.35

CV = coefficient of variation, SD = standard deviation, NO_3-*N* = nitrate concentration, calculated as nitrogen, NO_2-*N* = nitrite concentration, calculated as nitrogen, NH_4-*N* = ammonium concentration, calculated as nitrogen.

mainly distributed in three towns, namely Fengshan Town, Shuanglu Town and Xiangfu Town (Figure 2(d)). According to QSGC, approximately 36.36% of TDS samples exceed Class III values (Figure 3).

There are significant differences between the anion and cation of the concentrations in groundwater. The concentrations of SO_4^{2-}, Cl^-, and HCO_3^- in the groundwater are in the ranges of 0.21–448.97, 0.13–317.38 and 34.67–809.00 mg/L, respectively (Table 3). In shallow groundwater, the average concentration of anions is arranged in the following order: $HCO_3^- > Cl^- > SO_4^{2-}$. According to QSGC classification, 3.89% of SO_4^{2-} in groundwater samples exceeded Grade III levels (>250.00 mg/L; Figure 3), and 6.49% of Cl^- in groundwater samples exceeded Grade III levels (>250.00 mg/L) mg/L; Figure 3). As shown in Table 3, the concentrations of Ca^{2+}, K^+, Na^+, and Mg^{2+} in groundwater are in the ranges of 16.12–315.00, 0.76–41.17, 4.90–215.97, and 3.75–70.37 mg/L, respectively. The average concentrations of cations in shallow groundwater are arranged in the order of $Ca^{2+} > Na^+ > Mg^{2+} > K^+$.

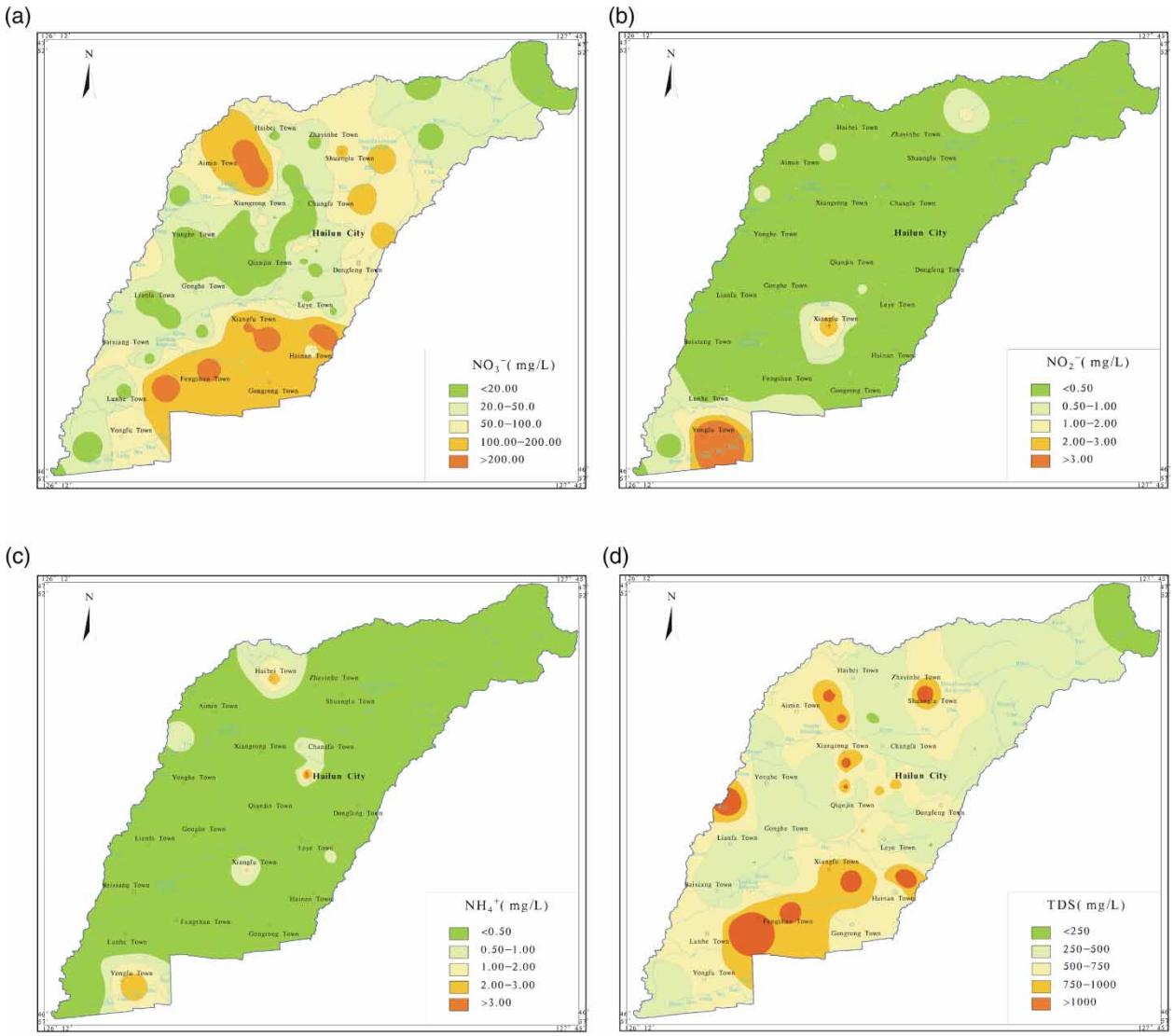

Figure 2 | Spatial distributions of groundwater chemical indexes (NO_3^-, NO_2^-, NH_4^+, and TDS).

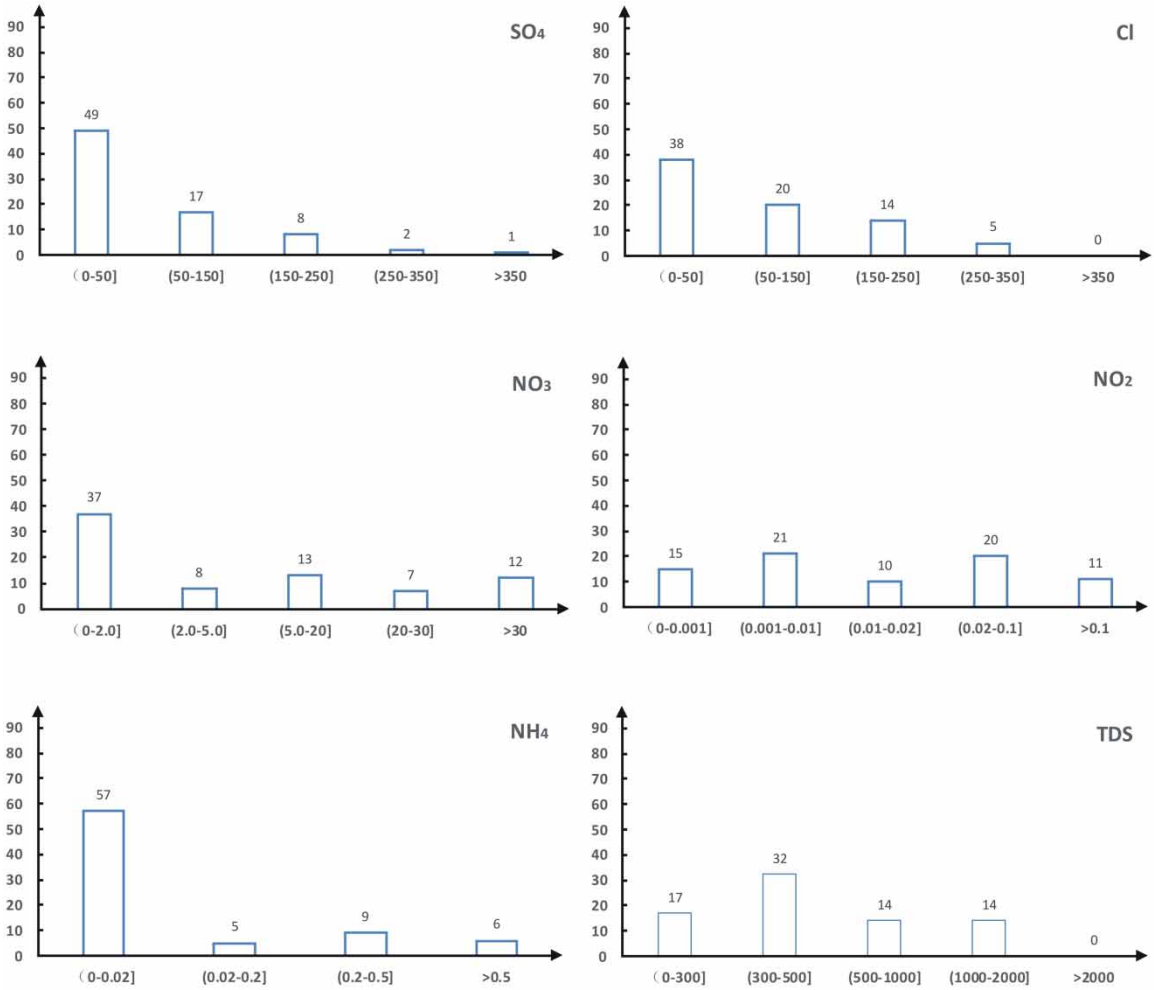

Figure 3 | Bar charts of different anions in groundwater chemical indexes.

Table 3 | The correlation coefficients of groundwater chemical indices in the study area

Parameter	pH	TDS	Ca^{2+}	Mg^{2+}	K +	Na^{+}	Cl^{-}	SO_4^{2-}	HCO_3^{-}	NO_3^{-}	NO_2^{-}	NH_4^{+}
pH	1.00											
TDS	−0.30	1.00										
Ca^{2+}	−0.28	**0.97**	1.00									
Mg^{2+}	−0.34	**0.91**	**0.88**	1.00								
K^{+}	−0.09	0.51	0.44	0.48	1.00							
Na^{+}	−0.06	**0.78**	**0.69**	0.65	0.47	1.00						
Cl^{-}	−0.51	**0.83**	**0.83**	**0.83**	0.41	0.58	1.00					
SO_4^{2-}	−0.22	**0.89**	**0.83**	**0.71**	0.50	**0.83**	0.67	1.00				
HCO_3^{-}	−.30	0.40	0.41	0.41	0.13	0.53	0.10	0.39	1.00			
NO_3^{-}	−0.25	**0.75**	0.65	0.68	0.55	0.60	0.54	0.64	0.08	1.00		
NO_2^{-}	−0.06	0.09	0.14	0.05	−0.04	0.05	0.02	0.08	0.10	0.10	1.00	
NH_4^{+}	0.03	−0.07	−0.05	−0.05	−0.06	−0.05	−0.06	−0.02	0.02	−0.09	0.40	1.00

Groundwater nitrate pollution

In recent years, nitrogen pollution of groundwater (NO_3-N, NO_2-N and NH_4-N) has become one of the main factors affecting groundwater quality (Rahmati *et al.* 2019). NO_3-N concentrations ranged from 0.00 to 112.42 mg/L with an average of 14.32 mg/L. According to WHO guidelines, the limited concentration for NO_3-N in water is 10 mg/L. According to QSGC classification, 24.67% of groundwater samples exceeded Grade III levels (20.00 mg/L of N; Figure 3). The spatial distribution of NO_3-N concentrations greater than 200 mg/L are mainly distributed in Fengshan Town, Aimin Town and Xiangfu Town (Figure 2(a)). NO_2-N concentrations ranged from 0.00 to 2.23 mg/L with an average of 0.09 mg/L. Concentrations in 40.26% of groundwater samples exceeded Grade III levels (0.02 mg/L of N; Figure 3). According to WHO guidelines, the allowable concentration for NO_2-N is 3 mg/L. The spatial distribution of NO_2-N concentrations greater than 3 mg/L is mainly distributed in Yongfu Town (Figure 2(b)).

The concentration of NH_4-N ranged from 0 to 4.01 mg/L, with an average of 0.18 mg/L. The concentrations in 80.52% of the groundwater samples were less than the Grade III levels (0.2 mg/L; Figure 3), reflecting a relatively stable spatial distribution (Figure 2(c)). According to WHO guidelines, the allowable concentration for NH_4-N in water is 0.3 mg/L. The increase of nitrate concentration is closely related to the use of chemical fertilizers and the infiltration of surface nitrogen (Chitsazan *et al.* 2019).

Durov diagram and groundwater hydrochemical types

The Durov diagram drawn by MapGIS software is used to reflect and describe the groundwater chemical characteristics of the study area (Mgbenu & Egbueri 2019). The upper triangle consisting of the main anions (SO_4^{2-}, Cl^- and HCO_3^-) is divided into four regions: A (sulfate type), B (chloride type), C (bicarbonate type) and D mixed type); Similarly, the left triangle consisting of the main cations is also divided into four regions: E (calcium type), F (magnesium type), G (sodium type) and H (mixed type). The chemical difference between anions and cations in groundwater is shown in Figure 4. The pH of the groundwater sample is around 7.0, and the TDS of the sample is concentrated at 300–500 mg/L. For the main anions of groundwater samples, the number of water samples falling in areas A, B, C and D was 0, 16, 17, and 44, respectively. Most of the samples are plotted in the D field, indicating that the anions in groundwater are dominated by mixed types. The blue filled circles in the field of C belonged to

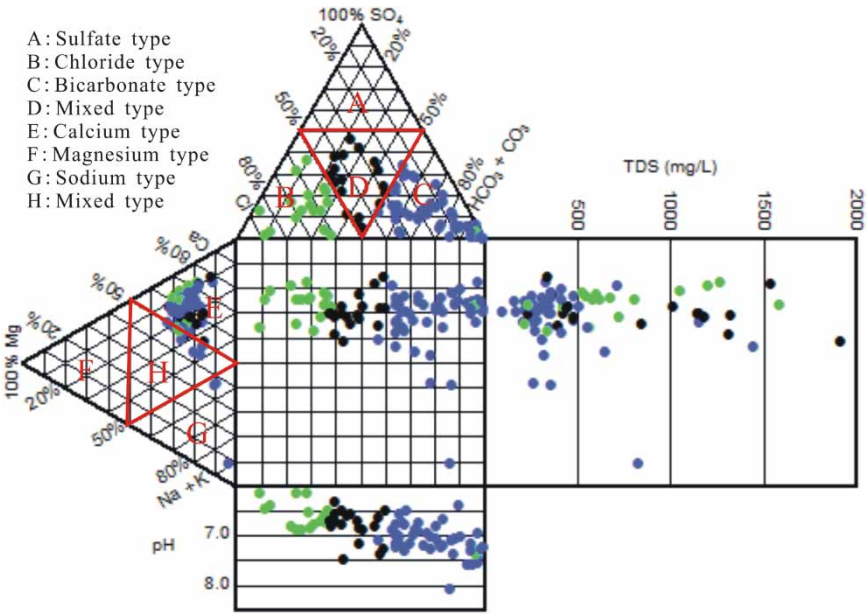

Figure 4 | Durov diagram of groundwater samples.

the bicarbonate type, indicating the dominant anion of HCO_3. For the main cations of groundwater samples, the number of water samples falling in areas E, F, G and H was 67, 0, 3, and 9, respectively. Most of the samples were plotted in the field of E, suggesting the dominance of Ca^{2+} in the groundwater. In summary, HCO_3 and Cl are the main anions in groundwater, while Ca and Na are the main cations. The groundwater in the shallow aquifer in Hailun area is mainly controlled by HCO_3-Ca, HCO_3•Cl-Ca, HCO_3-Ca•Na and HCO_3•Cl-Ca•Na types.

Silicate weathering

In 1970, Gibbs used the Gibbs plot to quantitatively analyze the evolution of surface water. Subsequently, the Gibbs plot is widely used to study the relationship between groundwater hydrochemistry and aquifer lithology (Ramachandran *et al.* 2019). A Gibbs diagram is divided into three parts, each of which reveals an evolutionary mechanism: evaporation dominance, rock dominance and precipitation dominance. As shown in Figure 5, the ratio of $Cl^-/(Cl^- + HCO_3^-)$, $(Na^+ + K^+)/(Na^+ + K^+ + Ca^{2+})$ and TDS is plotted. Most of the samples are plotted in the middle part of the diagrams, indicating that all of the samples (77 samples) are dominated by rock weathering and dissolution. The results show that rock weathering and dissolution controls the ionic composition of groundwater in this area. Groundwater chemistry is less affected by precipitation and evaporation, indicating that the groundwater level in the study area is buried deeper and groundwater is less affected by evaporation.

The relationship between Na^+ and Cl^- in Figure 6 can show the degree of the enrichment of Na^+ in groundwater samples. In general, if the ratio of Na^+ vs Cl^- is approximately equal to 1, the dissolution of the hydrochloride is the only source of Na^+ (Banks & Banks 2019). The ratios of Na^+ vs Cl^- in the study area varied from 0.14 to 189.63, with a mean value of 8.08, which means that there is another possible source of Na^+. About 82% of the samples are below the 1:1 line, indicating that they may be affected by both human activities and silicate weathering. The ratios of $(Ca^{2+} + Mg^{2+})$ vs HCO_3^- in the study area varied from 0.74 to 10.87, with a mean value of 2.17, which means that Ca^{2+} and Mg^{2+} also participate in another non-carbonate chemical reaction. About 74% of the samples are below the 1:1 line, indicating that the excess Ca^{2+} and Mg^{2+} may react with Cl^- to materialize non-carbonate salts, such as $CaCl_2$ and $MgCl_2$. The chemical formula of silicate can be expressed as $NaAlSi_3O_8$. The weathering and dissolution process of silicate under weakly alkaline conditions is shown in Equation (9) (Adimalla *et al.* 2019a, 2019b). Excessive Ca^{2+} and Mg^{2+} can exchange Na^+ from the minerals in the aquifer, causing the concentration of Na^+ to increase in groundwater. The exchange adsorption

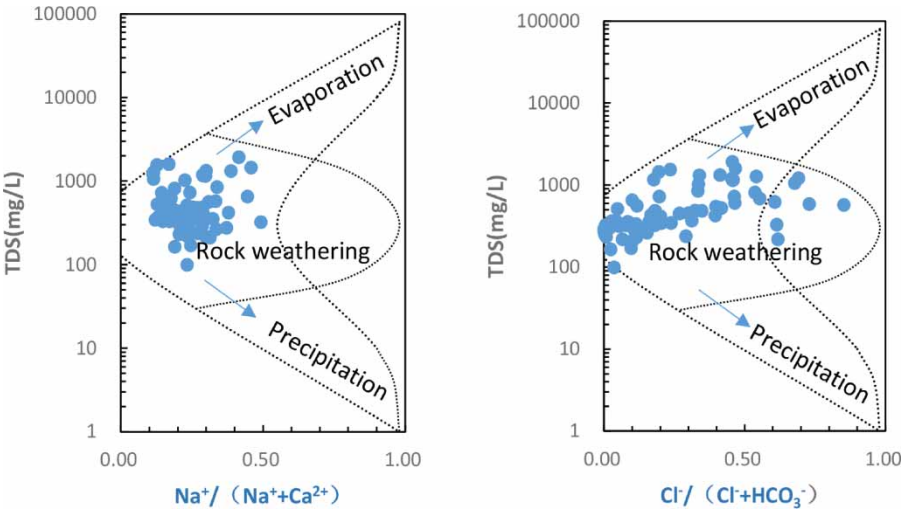

Figure 5 | The Gibbs plot of the groundwater samples.

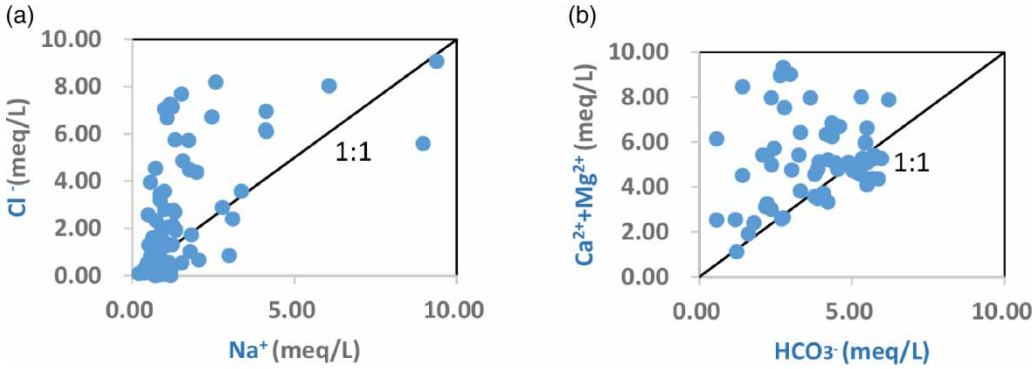

Figure 6 | The plot of the ratio of Na^+ vs Cl^- (a), $Ca^{2+} + Mg^{2+}$ vs HCO_3^- (b).

of Ca^{2+} and Mg^{2+} with Na^+ is also an important source of Na^+ in groundwater (Karunanidhi *et al.* 2020).

$$2NaAlSi_3O_8 + 2CO_2 + 11H_2O \rightarrow 2Na^+ + 2HCO_3^- + Al_2Si_2O_5(OH)_4 + 4H_4SiO_4 \quad (9)$$

Ion exchange

Ion exchange has a significant impact on the chemical properties of groundwater. The ratio of $Ca^{2+} + Mg^{2+}$-SO_4^{2-}-HCO_3^- (meq/L) and Na^+-Cl^- (meq/L) is close to –1, indicating that the dissolution of calcite, dolomite, and gypsum is the main form of water–rock interaction (Li *et al.* 2019). Figure 7 can better describe the process of ion exchange in the groundwater. The ratios of $Ca^{2+} + Mg^{2-}$-SO_4^2-HCO_3^- (meq/L) and Na^+-Cl^- (meq/L) in the groundwater range from –6.59 to 10.54, with an average value of –0.49, which means that the ions in groundwater exchange strongly with the ions on the surface of the aquifer rocks (Chitsazan *et al.* 2019) (Equations (10) and (11)):

$$Ca^{2+}(\text{groundwater}) + 2Na^+(\text{rock}) \rightleftharpoons Ca^{2+}(\text{rock}) + 2Na^+(\text{groundwater}) \quad (10)$$

$$Mg^{2+}(\text{groundwater}) + 2Na^+(\text{rock}) \rightleftharpoons Mg^{2+}(\text{rock}) + 2Na^+(\text{groundwater}) \quad (11)$$

Carbonate and sulfate dissolution

The chemical formula of calcite can be expressed as $CaCO_3$. As shown in the scatter diagrams of Ca^{2+}+ Mg^{2+} vs $HCO_3^- + SO_4^{2-}$, about 79.22% of the sampling points fall below 10 (Ca^{2+}+ $Mg^{2+} < 10$) meq/L, indicating that the dissolution of calcite is dominant (Figure 8, Equation (12)) (Yuan *et al.* 2020). The chemical formula

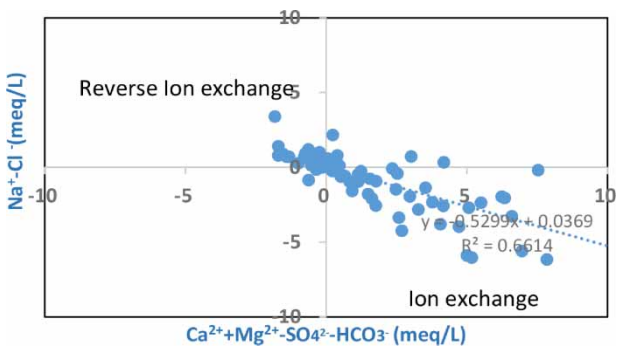

Figure 7 | The plot of the ratio of $Ca^{2+} + Mg^{2+}$-SO_4^2-HCO_3^- vs Na^+-Cl^-.

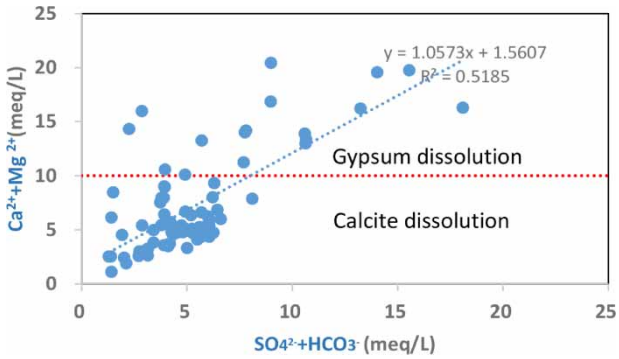

Figure 8 | The plot of the ratio of $SO_4^{2-} + HCO_3^-$ vs $Ca^{2+} + Mg^{2+}$.

of gypsum can be expressed as $CaSO_4$. Groundwater rich in calcium and sulfate is partially derived from the dissolution of gypsum ($CaSO_4{\cdot}2H_2O$) (Equation (13)). The plot of Ca^{2+}/SO_4^{2-} vs Cl^- (meq/L) also confirms this conclusion, and most of the groundwater samples fall above the unit line, indicating that the effect of gypsum dissolution on groundwater chemistry is very small (Figure 9). These reactions usually occur in the recharge area of many sedimentary aquifer environments (Lyu *et al.* 2019):

$$CaCO_3 + CO_2 + H_2O \rightarrow Ca^{2+} + 2HCO_3^- \quad (12)$$

$$CaSO_4{\cdot}2H_2O \rightarrow Ca^{2+} + SO_4^{2-} + 2H_2O \quad (13)$$

Factor and principal component analyses

Factor analysis and correlation analysis can help determine the source and correlation of ions in groundwater. As indicated in Table 4, TDS has a significant positive correlation with Na^+, Ca^{2+}, Mg^{2+}, NO_3^-, SO_4^{2-}, and Cl^-, suggesting that the spatial distribution of TDS is mainly affected by Na^+, Ca^{2+}, Mg^{2+}, NO_3^-, SO_4^{2-}, and Cl^- (Selvakumar *et al.* 2017a, 2017b). Besides, the high correlation between TDS and NO_3^- indicates that human activities, especially the use of chemical fertilizers, is one of the important reasons for the change of TDS in groundwater. The presence of NO_3^-, Mg^{2+} and SO_4^{2-} in this factor group simultaneously confirms the contribution of agricultural activities to its hydrochemical process (Selvakumar *et al.* 2017a, 2017b). The high correlation between Ca^{2+}, Mg^{2+} and Cl^- indicates that ion exchange is one of the causes for their high concentration. The high correlation between Ca^{2+} and SO_4^{2-} indicates that the dissolution of gypsum affects the concentration of Ca^{2+} and SO_4^{2-} in groundwater (Guo *et al.* 2019). Therefore, it is presumed that the main ions of groundwater in the study area are affected by the dissolution of aluminosilicate minerals, the dissolution of gypsum, ion exchange, and human activities.

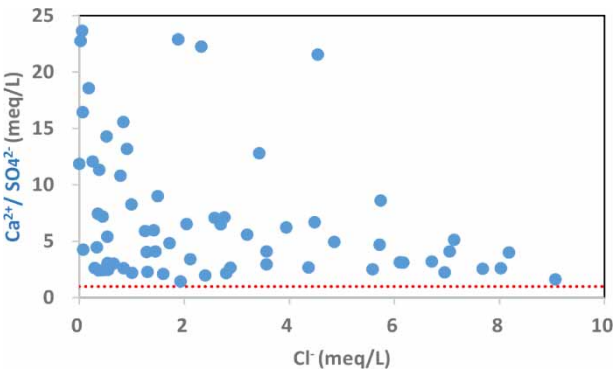

Figure 9 | The plot of the ratio of Ca^{2+}/SO_4^{2-} vs Cl^-.

HEALTH RISK ASSESSMENT

According to the USEPA groundwater quality standards and the corresponding HQ calculation results, the quality classification of NO_3-N is shown in Table 4. The HQ value for adult males, adult females, children, and infants were in the range of 0–1.52, 0–1.75, 0–3.58, and 0–6.08, respectively, and with a mean value of 0.19, 0.22, 0.44, and 0.75, respectively. It can be concluded that for health risks from NO_3^- pollution in groundwater, the harm is in the order of infant > child > adult female > adult male. This shows that minors in the study area are significantly more at risk of NO_3 pollution than adults. The increased harm to minors can be attributed to higher gastrointestinal absorption rates associated with groundwater-related activities, and increased sensitivity per unit weight to environmental pollutants.

According to the calculation results of HQ, a spatial distribution map is drawn of the health risk assessment in the study area for infants, children, adult females, and adult males (Figure 10). For adult males and females, the health risks from nitrate (HQ > 1) are mainly concentrated in the south (Hainan Town) and north (Aimin Town) of the study area, which accounts for about 5.60% of the total area, while for children and infants, the health risks from nitrate (HQ > 1) are mainly distributed in the south (Hainan Town, Gongrong Town, Xiangfu Town, and Fengshan Town) and north (Aimin Town and Shuanglu Town) of the study area, which accounts for about 27.41% of the total area.

It is worth noting that areas with high health risks of NO_3^- are distributed in agricultural production areas,

Table 4 | Health risk assessment of nitrogen (NO_3-N) based on USEPA

	HQ(NO_3-N)					HQ(NO_3-N)			
Sample	**Males**	**Females**	**Children**	**Infant**	**Sample**	**Males**	**Females**	**Children**	**Infant**
GW01	0.03	0.03	0.07	0.11	GW40	0.54	0.63	1.28	2.17
GW02	0.08	0.09	0.19	0.33	GW41	0.22	0.25	0.51	0.86
GW03	0.01	0.01	0.02	0.03	GW42	0.42	0.49	1.00	1.69
GW04	0.16	0.19	0.38	0.65	GW43	0.13	0.15	0.30	0.50
GW05	0.10	0.12	0.24	0.40	GW44	0.32	0.37	0.76	1.30
GW06	0.04	0.04	0.09	0.15	GW45	0.16	0.18	0.37	0.62
GW07	0.01	0.01	0.03	0.05	GW46	1.45	1.67	3.41	5.79
GW08	0.37	0.43	0.88	1.49	GW47	0.13	0.15	0.30	0.52
GW09	0.03	0.04	0.07	0.13	GW48	0.01	0.01	0.02	0.04
GW10	0.00	0.00	0.00	0.00	GW49	0.01	0.01	0.03	0.04
GW11	0.01	0.01	0.02	0.03	GW50	0.00	0.00	0.00	0.01
GW12	0.03	0.03	0.07	0.11	GW51	0.10	0.11	0.22	0.38
GW13	0.01	0.01	0.03	0.05	GW52	0.00	0.00	0.01	0.01
GW14	0.28	0.32	0.66	1.12	GW53	0.00	0.01	0.01	0.02
GW15	0.01	0.01	0.01	0.02	GW54	0.27	0.31	0.63	1.08
GW16	0.00	0.00	0.00	0.00	GW55	0.01	0.01	0.02	0.03
GW17	0.01	0.01	0.02	0.04	GW56	0.97	1.11	2.27	3.86
GW18	0.00	0.00	0.00	0.00	GW57	0.00	0.00	0.01	0.01
GW19	0.02	0.02	0.05	0.08	GW58	0.00	0.00	0.00	0.00
GW20	0.02	0.02	0.05	0.08	GW59	0.16	0.18	0.37	0.63
GW21	0.01	0.01	0.01	0.02	GW60	0.00	0.00	0.00	0.00
GW22	0.00	0.00	0.00	0.00	GW61	0.00	0.00	0.01	0.01
GW23	0.18	0.21	0.43	0.72	GW62	1.07	1.23	2.52	4.28
GW24	0.00	0.00	0.00	0.00	GW63	0.31	0.35	0.72	1.22
GW25	0.00	0.00	0.00	0.00	GW64	0.01	0.01	0.03	0.04
GW26	0.00	0.00	0.00	0.00	GW65	1.52	1.75	3.58	6.08
GW27	0.02	0.02	0.04	0.07	GW66	0.55	0.63	1.30	2.20
GW28	0.30	0.34	0.70	1.19	GW67	0.79	0.91	1.87	3.17
GW29	0.06	0.06	0.13	0.22	GW68	0.79	0.91	1.87	3.17
GW30	0.03	0.03	0.07	0.12	GW69	0.00	0.00	0.00	0.00
GW31	0.05	0.06	0.12	0.20	GW70	0.67	0.77	1.57	2.66
GW32	0.01	0.01	0.02	0.03	GW71	0.91	1.04	2.13	3.62
GW33	0.36	0.41	0.85	1.44	GW72	0.01	0.01	0.01	0.02
GW34	0.13	0.15	0.30	0.51	GW73	0.00	0.00	0.00	0.00
GW35	0.02	0.02	0.04	0.07	GW74	0.29	0.34	0.69	1.17
GW36	0.00	0.00	0.01	0.02	GW75	0.04	0.04	0.09	0.16
GW37	0.01	0.01	0.02	0.04	GW76	0.00	0.00	0.00	0.00
GW38	0.43	0.49	1.01	1.71	GW77	0.00	0.00	0.00	0.00
GW39	0.25	0.29	0.60	1.01					

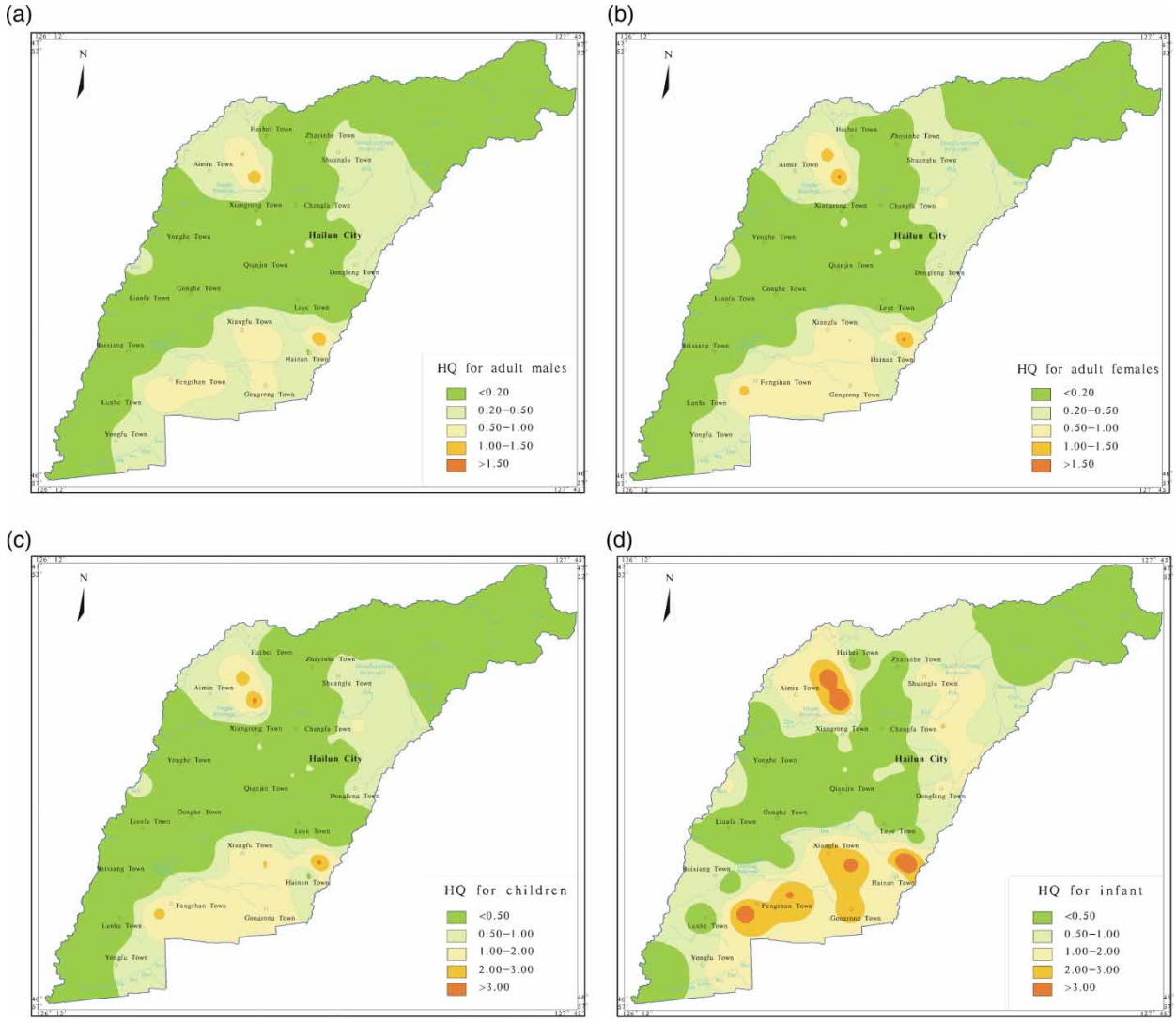

Figure 10 | The spatial distribution map of the risk based on the HHRA model.

especially rice cultivation areas (the middle and lower reaches of the Zhayin River, the upper reaches of the Helen River, and the middle reaches of the Sandaowulong River). The large-scale use of nitrogen fertilizer and irrigation of domestic sewage are the main reasons for the increased health risk of NO_3^-. Therefore, the local government should strengthen the management of groundwater resources and prevent and control the nitrate pollution of groundwater to ensure the safety of drinking water for the local residents.

CONCLUSIONS

This study explored the factors affecting groundwater chemistry, and analyzed the hydrogeological processes of shallow groundwater. Human health risk assessment of nitrate contamination was also performed in accordance with USEPA2004 guidelines. The following three conclusions were established:

1. The abundance for groundwater is in the order $Ca^{2+} > Na^+ > Mg^{2+}$ for cations, and $HCO_3^- > Cl^- > SO_4^{2-}$ for

anions, resulting in that the water types were dominated by HCO_3-Ca, HCO_3•Cl-Ca, HCO_3-Ca•Na and HCO_3•Cl-Ca•Na types. Groundwater in the study area is weakly acidic.

2. Groundwater hydrochemistry shows that rock weathering and dissolution, ion exchange, and human activities are the main reasons affecting the chemical composition of shallow groundwater in Hailun. The weathering and dissolution process of silicate under weakly alkaline conditions is the source of Na^+. The dissolution of calcite, dolomite, and gypsum is the main form of water–rock interaction.
3. The HQ values for adult males, adult females, children, and infants were in range of 0–1.52, 0–1.75, 0–3.58, and 0–6.08, respectively, and with a mean value of 0.19, 0.22, 0.44, and 0.75, respectively. The harm of NO_3^- pollution is in the order of infant > child > adult female > adult male. The health risks from NO_3^- (HQ > 1) are mainly distributed in the Hainan Town and Aimin Town of the study area for adult males and females, while that for children and infants was distributed in the towns of Hainan, Gongrong, Xiangfu, Fengshan, Aimin and Shuanglu.

For human health and the sustainable development of groundwater resources, the following three suggestions are proposed: (1) residents living in the towns of Hainan, Gongrong, Xiangfu, Fengshan, Aimin and Shuanglu are advised to prohibit drinking and mining groundwater; (2) recommend the use of surface water for irrigation, restricting the exploitation of groundwater; (3) reduce the use of chemical fertilizers and fertilize according to the needs of the soil. The results of this study made local governments pay attention to drinking water safety issues for local residents.

ACKNOWLEDGEMENTS

This work was supported by the projects of hydrological and geological survey in Hailun, Bayan and Wuhe Area (Item Number: DD20190340-1). Thanks are extended to Yonggen Zhang, Shanghai Du, and Xiaoqing Sun for helping with mapping and writing skills in the process of writing this paper. We are also grateful to valuable comments and suggestions given by the editors and the anonymous reviewers.

DATA AVAILABILITY STATEMENT

All relevant data are included in the paper or its Supplementary Information.

REFERENCES

Adimalla, N., Li, P. & Qian, H. 2019a Evaluation of groundwater contamination for fluoride and nitrate in semi-arid region of Nirmal Province, South India: a special emphasis on human health risk assessment (HHRA). *Human Ecol. Risk Assess. Int. J.* **25** (5), 1107–1124.

Adimalla, N., Marsetty, S. K. & Xu, P. 2019b Assessing groundwater quality and health risks of fluoride pollution in the Shasler Vagu (SV) watershed of Nalgonda, India. *Human Ecol. Risk Assess. Int. J.* **26** (6), 1–20.

Banks, P. J. & Banks, J. C. 2019 Relationship between soil and groundwater salinity in the Western Canada Sedimentary Basin. *Environ. Monit. Assess.* **191** (12), 761–780.

Chen, J., Wu, H., Qian, H. & Li, X. 2018 Challenges and prospects of sustainable groundwater management in an agricultural plain along the Silk Road Economic Belt, north-west China. *International J. Water Resour. Dev.* **34** (3), 354–368.

Chitsazan, M., Aghazadeh, N., Mirzaee, Y. & Golestan, Y. 2019 Hydrochemical characteristics and the impact of anthropogenic activity on groundwater quality in suburban area of Urmia city, Iran. *Environ. Dev. Sustain.* **21** (1), 331–351.

DellaValle, C. T., Xiao, Q., Yang, G., Shu, X. O., Aschebrook-Kilfoy, B., Zheng, W. & Gao, Y. T. 2014 Dietary nitrate and nitrite intake and risk of colorectal cancer in the Shanghai Women's Health Study. *Int. J. Cancer* **134** (12), 2917–2926.

De Roos, A. J., Ward, M. H., Lynch, C. F. & Cantor, K. P. 2003 Nitrate in public water supplies and the risk of colon and rectum cancers. *Epidemiology* **14** (6), 640–649.

Duggal, V., Mehra, R. & Rani, A. 2013 Determination of 222RN level in groundwater using a RAD7 detector in the Bathinda district of Punjab, India. *Radiat. Prot. Dosim.* **156**, 239–245.

Ford, L., Bharadwaj, L., McLeod, L. & Waldner, C. 2017 Human health risk assessment applied to rural populations dependent on unregulated drinking water sources: a scoping review. *Int. J. Environ. Res. Public Health* **14** (8), 846–868.

Guo, X., Zuo, R., Wang, J., Meng, L., Teng, Y., Shi, R. & Ding, F. 2019 Hydrogeochemical evolution of interaction between surface water and groundwater affected by exploitation. *Groundwater* **57** (3), 430–442.

Harries, S. & Harper, B. 2004 *Exposure Scenario for CTUIR Traditional Subsistence Lifeways, Confederated Tribes of the Umatilla Indian Reservation*. Department of Science and Engineering, Pendleton, Oregon.

Jha, M. K., Chowdhury, A., Chowdary, V. M. & Peiffer, S. 2007 Groundwater management and development by integrated remote sensing and geographic information systems: prospects and constraints. *Water Resour. Manage.* **21** (2), 427–467.

Jones, R. R., DellaValle, C. T., Weyer, P. J., Robien, K., Cantor, K. P., Krasner, S. & Ward, M. H. 2019 Ingested nitrate, disinfection by-products, and risk of colon and rectal cancers in the Iowa Women's Health Study cohort. *Environ. Int.* **126**, 242–251.

Karunanidhi, D., Aravinthasamy, P., Deepali, M., Subramani, T. & Roy, P. D. 2020 The effects of geochemical processes on groundwater chemistry and the health risks associated with fluoride intake in a semi-arid region of South India. *RSC Adv.* **10** (8), 4840–4859.

Kumar, D., Singh, A., Jha, R. K., Sahoo, B. B., Sahoo, S. K. & Jha, V. 2019 Source characterization and human health risk assessment of nitrate in groundwater of middle Gangetic Plain, India. *Arab. J. Geosci.* **12** (11), 339–350.

Li, P., Wu, J., Qian, H., Lyu, X. & Liu, H. 2014 Origin and assessment of groundwater pollution and associated health risk: a case study in an industrial park, northwest China. *Environ. Geochem. Health* **36** (4), 693–712.

Li, X., Li, J., Fang, X., Gong, Y. & Wang, W. 2016 Case studies of the sponge city program in China. In: *World Environmental and Water Resources Congress 2016*. (C. S. Pathak & D. Reinhart, eds). Department of Civil Engineering, Auburn University, Auburn, pp. 295–308.

Li, X. H., Wang, R. & Li, J. F. 2018 Study on hydrochemical characteristics and formation mechanism of shallow groundwater in eastern Songnen Plain. *J. Groundwater Sci. Eng.* **5** (3), 161–170.

Li, P., He, X., Li, Y. & Xiang, G. 2019 Occurrence and health implication of fluoride in groundwater of loess aquifer in the Chinese loess plateau: a case study of Tongchuan, Northwest China. *Expo. Health* **11** (2), 95–107.

Luo, L., Mao, D., Wang, Z., Du, B., Yan, H. & Zhang, B. 2018 Remote sensing and GIS support to identify potential areas for wetland restoration from cropland: a case study in the west Songnen plain, Northeast China. *Sustainability* **10** (7), 2375–2389.

Lyu, M., Pang, Z., Yin, L., Zhang, J., Huang, T., Yang, S. & Gulbostan, T. 2019 The control of groundwater flow systems and geochemical processes on groundwater chemistry: a case study in Wushenzhao Basin, NW China. *Water* **11** (4), 790–813.

Ma, Y., Egodawatta, P., McGree, J., Liu, A. & Goonetilleke, A. 2016 Human health risk assessment of heavy metals in urban stormwater. *Sci. Total Environ.* **557**, 764–772.

Mgbenu, C. N. & Egbueri, J. C. 2019 The hydrogeochemical signatures, quality indices and health risk assessment of water resources in Umunya district, southeast Nigeria. *Appl. Water Sci.* **9** (1), 22–41.

Peiyue, L., Qian, W. & Jianhua, W. 2011 Groundwater suitability for drinking and agricultural usage in Yinchuan Area, China. *Int. J. Environ. Sci.* **1** (6), 1241–1249.

Qiu, B., Lu, D., Tang, Z., Chen, C. & Zou, F. 2017 Automatic and adaptive paddy rice mapping using landsat images: case study in songnen plain in northeast China. *Sci. Total Environ.* **598**, 581–592.

Raeisi, A., Bijani, M. & Chizari, M. 2018 The mediating role of environmental emotions in transition from knowledge to sustainable use of groundwater resources in Iran's agriculture. *Int. Soil Water Conserv. Res.* **6** (2), 143–152.

Rahmati, O., Choubin, B., Fathabadi, A., Coulon, F., Soltani, E., Shahabi, H. & Bui, D. T. 2019 Predicting uncertainty of machine learning models for modelling nitrate pollution of groundwater using quantile regression and UNEEC methods. *Sci. Total Environ.* **688**, 855–866.

Ramachandran, A., Krishnamurthy, R. R., Jayaprakash, M. & Shanmugasundharam, A. 2019 Environmental impact assessment of surface water and groundwater quality due to flood hazard in Adyar River Bank. *Acta Ecol. Sin.* **39** (2), 125–132.

Rani, A., Mehra, R., Duggal, V. & Balaram, V. 2013 Analysis of uranium concentration in drinking water samples using ICPMS. *Health Phys.* **104**, 251–255.

Rizeei, H. M., Pradhan, B., Saharkhiz, M. A. & Lee, S. 2019 Groundwater aquifer potential modeling using an ensemble multi-adoptive boosting logistic regression technique. *J. Hydrol.* **579**, 124172.

Schullehner, J., Hansen, B., Thygesen, M., Pedersen, C. B. & Sigsgaard, T. 2018 Nitrate in drinking water and colorectal cancer risk: a nationwide population-based cohort study. *Int. J. Cancer* **143** (1), 73–79.

Selvakumar, S., Chandrasekar, N. & Kumar, G. 2017a Hydrogeochemical characteristics and groundwater contamination in the rapid urban development areas of Coimbatore, India. *Water Resour. Ind.* **17**, 26–33.

Selvakumar, S., Ramkumar, K., Chandrasekar, N., Magesh, N. S. & Kaliraj, S. 2017b Groundwater quality and its suitability for drinking and irrigational use in the Southern Tiruchirappalli district, Tamil Nadu, India. *Appl. Water Sci.* **7** (1), 411–420.

Su, X. S., Wang, H. & Zhang, Y. L. 2013 Health risk assessment of nitrate contamination in groundwater: a case study of an agricultural area in northeast China. *Water Resour. Manage.* **27**, 3025–3034.

Tian, H., Liang, X., Gong, Y., Kang, Z. & Jin, H. 2019 Health risk assessment of nitrate pollution in shallow groundwater: a case study in Changchun New District, China. *La Houille Blanche* **5–6**, 45–58.

Tian, H., Liang, X., Gong, Y., Ma, S., Kang, Z. & Jin, H. 2020a Risk assessment of metals from shallow groundwater in Lianhuashan District, China. *La Houille Blanche* **1**, 5–15. DOI: 10.1051/lhb/2019063.

Tian, H., Liang, X., Gong, Y., Qi, L., Liu, Q., Kang, Z. & Jin, H. 2020b Health risk assessment of nitrate pollution in shallow groundwater: a case study in China. *Pol. J. Environ. Stud.* **29** (1), 827–839.

USDOE 2011 *The Risk Assessment Information System (RAIS)*. U.S. Department of Energy's Oak Ridge Operations Office (ORO), Washington, DC, USA.

USEPA (US Environmental Protection Agency) 2004 *Risk ASSESSMENT GUIDANCE for Superfund*. Volume I: Human Health Evaluation Manual (Part E, Supplemental Guidance for Dermal Risk Assessment) Final. USEPA, USA.

Yang, Y., Zhang, Y., Yang, Q., Liu, J. & Huang, F. 2019 Coupling relationship between agricultural labor and agricultural production against the background of rural shrinkage: a case study of Songnen Plain, China. *Sustainability* **11** (20), 5804–5828.

Yuan, R., Wang, M., Wang, S. & Song, X. 2020 Water transfer imposes hydrochemical impacts on groundwater by altering the interaction of groundwater and surface water. *J. Hydrol.* **583**, 124617–124620.

Zhai, Y. Z., Zhao, X. B., Teng, Y. G., Li, X., Zhang, J. J., Wu, J. & Zuo, R. 2017 Groundwater nitrate pollution and human health risk assessment by using HHRA model in an agricultural area, NE China. *Ecotoxicol. Environ. Saf.* **137**, 130–142.

Zhang, B., Song, X. F., Zhang, Y. H., Han, D. M., Tang, C. Y., Lihu, Y. A. N. G. & Wang, Z. L. 2017 The renewability and quality of shallow groundwater in Sanjiang and Songnen Plain, Northeast China. *J. Integr. Agric.* **16** (1), 229–238.

Zhang, Y., Wu, J. & Xu, B. 2018 Human health risk assessment of groundwater nitrogen pollution in Jinghui canal irrigation area of the loess region, northwest China. *Environ. Earth Sci.* **77** (7), 273–285.

Zhu, L., Gong, H., Li, X., Wang, R., Chen, B., Dai, Z. & Teatini, P. 2015 Land subsidence due to groundwater withdrawal in the northern Beijing plain, China. *Eng. Geol.* **193**, 243–255.

First received 25 February 2020; accepted in revised form 29 June 2020. Available online 9 October 2020